
[View Journal Online](#)
[View Article Online](#)

Rationalization of supramolecular interactions of a newly synthesized binuclear Cu(II) complex derived from 4,4',6,6'-tetramethyl 2,2'-bipyrimidine ligand through Hirshfeld surface analysis

 Samit Pramanik ¹, Subrata Mukhopadhyay ¹ and Kinsuk Das ^{2,*}
¹ Department of Chemistry, Jadavpur University, Kolkata 700032, West Bengal, India

² Department of Chemistry, Chandernagore College, Hooghly, West Bengal 712136, India

 * Corresponding author at: Department of Chemistry, Chandernagore College, Hooghly, West Bengal 712136, India.
 e-mail: kdaschem@yahoo.in (K. Das).

RESEARCH ARTICLE

ABSTRACT



doi 10.5155/eurjchem.13.4.393-401.2318

Received: 10 August 2022

Received in revised form: 12 September 2022

Accepted: 19 September 2022

Published online: 31 December 2022

Printed: 31 December 2022

KEYWORDS

 Hirshfeld surface
 Bipyrimidine derivative
 Lone pair... π interactions
 Supramolecular architectures
 Hydrogen bonding interactions
 Single crystal X-ray crystallography

A new binuclear copper (II) complex $[\text{Cu}_2\text{L}_2\text{Cl}_4(\text{H}_2\text{O})_2]$ (1) derived from 4,4',6,6'-tetramethyl-2,2'-bipyrimidine (L) has been synthesized and characterized by the single crystal X-ray diffraction method. Single crystal analysis of complex 1 reveals that it crystallizes in the space group $P2_1/n$ under a monoclinic system ($\beta = 97.995(2)^\circ$, $a = 7.6483(2)$, $b = 7.2158(3)$ and $c = 17.8477(6)$ Å). The ligand acts as a bis-bidentate one and each copper (II) center bears a square pyramidal geometry exploiting $\text{N}_2\text{Cl}_2\text{O}$ chromophore. In the solid state, the complex is stabilized through classical $\text{O-H}\cdots\text{Cl}$ intermolecular hydrogen bonding incorporating coordinated water (as a solvent) and chloride ions and lone pair... π interactions. The Hirshfeld surface analysis demonstrates $\text{H}\cdots\text{H}/\text{H}\cdots\text{H}$, $\text{H}\cdots\text{Cl}/\text{Cl}\cdots\text{H}$, $\text{H}\cdots\text{C}/\text{C}\cdots\text{H}$, and $\text{C}\cdots\text{Cl}/\text{Cl}\cdots\text{C}$ intermolecular interactions as the major contributor interactions in the solid-state packing of the molecular crystal. Interaction energy calculations carried out employing the wavefunction generated via B3LYP/6-31G(d,p) highlight the dominance of electrostatic energy and the contribution of polarization and dispersion energy towards the total energy of complex 1 in the solid state.

 Cite this: *Eur. J. Chem.* 2022, 13(4), 393-401

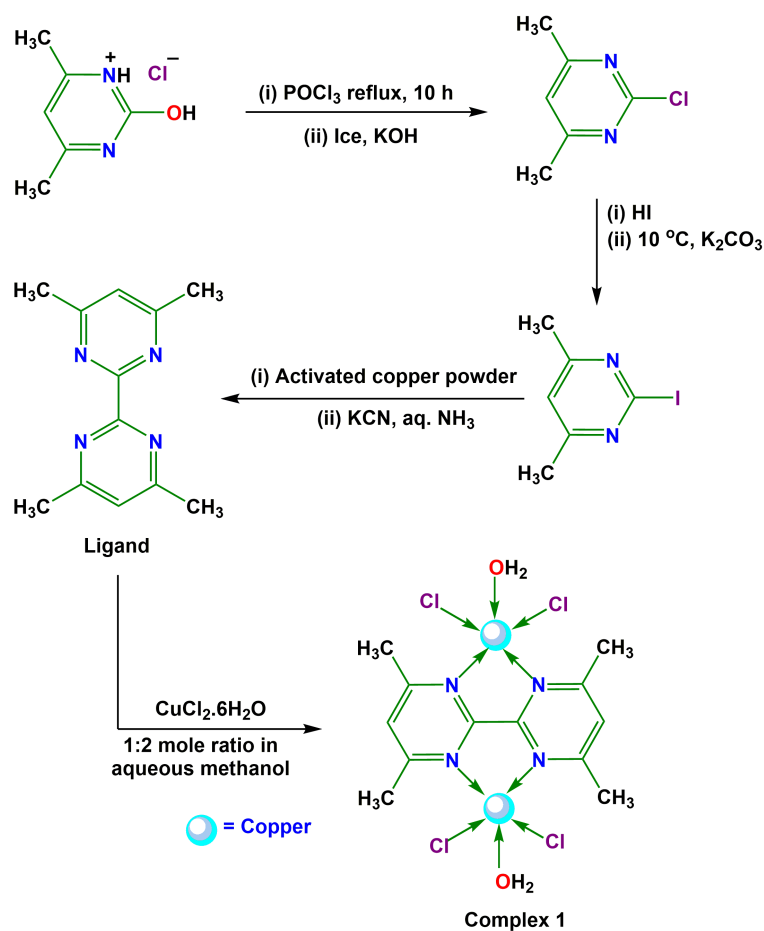
 Journal website: www.eurjchem.com

1. Introduction

Non-covalent interactions, namely, intra- and intermolecular hydrogen bonding, hydrophobic interactions, dispersion interactions, halogen bonding, carbon bonding, $\pi\cdots\pi$, cation... π , C-H... π , lone pair... π , salt bridge... π , anion... π etc. have arrested recent attention of the chemists as they play a pivotal role in the self-assembly of well-defined molecular components into tailor made large supramolecular aggregates [1-3]. Although the structure-directing role of weak noncovalent interactions was perceived about almost three decades ago, the discovery of new interactions with quantification still attracts interest as it is able to regulate molecular aggregation into supramolecular assembly [4-12]. The judicious choice of heterocyclic aromatic systems is very much important in the design and development of functional materials. Among heterocyclic polydentate nitrogen donor ligands, pyrimidine-derived ligands have attracted the attention of researchers due to their versatile application in various fields [11,12], especially in crystal engineering [13,14]. In the recent past, a new type of non-covalent supramolecular interaction involving an aromatic molecule (Homo- or hetero-cyclic) has been considered, namely, the binding association between anion or lone pair and

electron deficient aromatic ring. Such interactions can be exploited in synthetic anion receptors only when the aromatic system has sufficient π -acidity [15]. The higher π -acidity and the presence of more than one heteroatom in pyrimidine play an important role in this regard. 2,2'-Bipyrimidine has been widely used in the synthesis of metal complexes [15]. As a versatile ligand, it is able to coordinate metal ions in either strong bidentate or bis-bidentate bridging mode leading to mono-, di- or poly-nuclear complexes [15-18]. Extensive research has been devoted to the synthesis and study of bridged binuclear copper complexes with structural and functional diversities that include coordination chemistry, magnetism, material chemistry, and biology [19,20]. In 2009, Luo *et al.* [21] and in 2012 Marino *et al.* [22] had reported some Cu(II) complexes with 2,2'-bipyrimidine as a bridge ligand. In 2014, Ma *et al.* reported complexes of dicobalt [23] and dinickel [18] with 2,2'-bipyrimidine substituted with tetraphosphate.

To understand such a system, we succeeded in synthesizing a Cu(II) complex of 4,4',6,6'-tetramethyl-2,2'-bipyrimidine that is characterized by single-crystal X-ray analysis. Here, the title ligand acts as a bis-bidentate ligand and bridges two copper centers separated by a distance of 5.693 Å. As expected, the electron-deficient pyrimidine moiety (both nitrogen in the



Scheme 1. Schematic representation of the synthesis of ligand and complex 1.

pyrimidine ring is coordinated with the metal Cu(II) centers) participates in the lone pair $\cdots\pi$ interaction along with the intermolecular hydrogen bonding between hydrogen atoms of coordinated water molecules and coordinated chloride ions.

To the best of our knowledge, it is the first report of lone pair $\cdots\pi$ interactions present in a substituted bipyrimidine bridged binuclear Cu(II) complex. Such kind of supramolecular interactions help in enhancement of the dimensionality of the complex in the solid state. We have also performed a detailed investigation of the intermolecular interactions by Hirshfeld surface analysis. The contribution of each interaction to the formation of the self-assembly has been analyzed through a Hirshfeld surface calculation, which enables quantitative contributions to the crystal packing in a novel visual manner. The structural descriptions have been corroborated with theoretical calculations [24-27].

2. Experimental

All chemicals were of reagent grade, purchased from commercial sources and used without further purification. 4,6-Dimethyl-2-hydroxy pyrimidine hydrochloride was purchased from Aldrich Chemical Company, USA and used without further purification. All reactions were carried out in aerobic condition and in aqueous-methanol medium. The Perkin-Elmer RXI FT-IR spectrophotometer was used to record the IR spectra in the range of 4000-400 cm^{-1} and an elemental analysis (carbon, hydrogen, and nitrogen) of the metal complex was determined with a Perkin-Elmer CHN analyzer 2400. The mass spectrum of the ligand was performed with a JEOLJMS-AX 500 mass spectrophotometer.

2.1. Synthesis of protonated ligand (L)

The ligand L was synthesized using 4,6-dimethyl-2-hydroxy pyrimidine hydrochloride as the starting material and the synthesis was carried out following the procedure reported [28] as shown in Scheme 1. Yield: 59%. M.p.: 132-134 °C. FT-IR (KBr, ν , cm^{-1}): 2960, 2910 ($\nu_{\text{C-H}}$, CH₃), 1575 ($\nu_{\text{C=N}}$), 1497 ($\nu_{\text{C=C}}$), 1358, 1093 (Ring str.), 802 ($\nu_{\text{C-H}}$), 637 (Ring bend.). Anal. calc. for C₁₂H₁₄N₄: C, 67.27; H, 6.59; N, 26.15. Found: C, 67.17; H, 6.49; N, 26.11%. MS (m/z (%)): 214 (M⁺, 100%).

2.2. Synthesis of [Cu₂L₂Cl₄(H₂O)₂] (Complex 1)

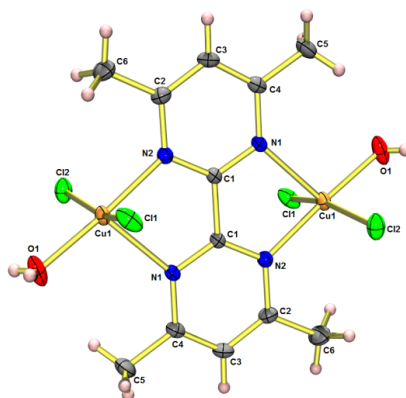
The aqueous methanolic solution of CuCl₂·6H₂O (0.485 g, 2 mmol) was added to the synthesized ligand (4,4',6,6'-tetramethyl-2,2'-bipyrimidine (L)) in the same solvent (0.214 g, 1 mmol). The mixture was stirred for 3 hours (Scheme 1) under aerial condition. The color of the solution turned blue and the solution was left for slow evaporation, and after two weeks a blue-colored X-ray quality crystal of complex 1 was isolated. Color: Blue. Yield: 67%. Anal. calc. for C₁₂H₁₈Cu₂N₄O₂Cl₄: C, 27.74; H, 3.46; N, 10.78. Found: C, 27.53; H, 3.39; N, 10.71. FT-IR (KBr, ν , cm^{-1}): 3443 ($\nu_{\text{O-H}}$), 2959, 2917 ($\nu_{\text{C-H}}$, CH₃), 1560 ($\nu_{\text{C=N}}$), 1519 ($\nu_{\text{C=C}}$), 1433, 1393 (Ring str.), 650, 643 (Ring bend.).

2.3. X-ray crystallographic analysis

Data collection was carried out using a Bruker SMART APEX II CCD area detector equipped with a graphite monochromated MoK α radiation ($\lambda = 0.71073 \text{ \AA}$) in φ and ω scan mode at 293 K for complex 1.

Table 1. Crystal data and structure refinement for complex **1**.

Empirical formula	C ₁₂ H ₁₈ Cl ₄ Cu ₂ N ₄ O ₂
Formula weight (g/mol)	519.20
Temperature (K)	293(2)
Crystal system	Monoclinic
Space group	P2 ₁ /n
a, (Å)	7.6483(2)
b, (Å)	7.2158(3)
c, (Å)	17.8477(6)
α (°)	90.00
β (°)	97.395(2)
γ (°)	90.00
Volume (Å ³)	976.80(6)
Z	2
ρ _{calc} (g/cm ³)	1.765
μ (mm ⁻¹)	2.736
F(000)	520.0
Crystal size (mm ³)	0.33 × 0.28 × 0.21
Radiation	MoKα (λ = 0.71073)
2θ range for data collection (°)	4.6 to 52.78
Index ranges	-9 ≤ h ≤ 9, -9 ≤ k ≤ 9, -22 ≤ l ≤ 22
Reflections collected	10093
Independent reflections	1986 [R _{int} = 0.0333, R _{sigma} = 0.0247]
Data/restraints/parameters	1986/0/145
Goodness-of-fit on F ²	1.031
Final R indexes [I ≥ 2σ (I)]	R ₁ = 0.0247, wR ₂ = 0.0596
Final R indexes [all data]	R ₁ = 0.0314, wR ₂ = 0.0626
Largest diff. peak/hole (e.Å ⁻³)	0.39/-0.26
CCDC no	2192141

**Figure 1.** Perspective view of complex **1**, displacement ellipsoids are drawn at 30% probability level.

Cell parameter refinement and data reduction were carried out using Bruker SMART and Bruker SAINT software [29]. The structure of the complex was solved by conventional direct methods and refined by full-matrix least squares method using F^2 data. The SHELXS-97 and SHELXL-97 programs [30] were used for the solution and refinement of the structure of the complex, respectively. CCDC 2192141 (**1**) includes additional crystallographic information. Selected crystallographic features for complex **1** are given in Table 1 and the selected metrical parameters of the complex are shown in Table 2. The molecular representation with atom numbering scheme (only selected atom numbering was done for maintaining the clarity of the picture) of complex **1** is shown in Figure 1.

2.4. Hirshfeld surface analysis

Hirshfeld surfaces [31-33] and the associated two-dimensional (2D) fingerprint [26,34-36] plots were calculated using CrystalExplorer [37] with bond lengths to hydrogen atoms set to standard values. Two distances, d_e (the distance from the point to the nearest nucleus external to the surface) and d_i (the distance to the nearest nucleus internal to the surface), are defined for each point on the Hirshfeld surface. The normalized contact distance (d_{norm}) based on d_e and d_i is defined as:

$$d_{norm} = \frac{(d_i - r_i^{vdw})}{r_i^{vdw}} + \frac{(d_e - r_e^{vdw})}{r_e^{vdw}} \quad (1)$$

where r_i^{vdw} and r_e^{vdw} are the van der Waals radii of the atoms. The d_{norm} value is negative or positive depending on intermolecular contacts being shorter or longer than the van der Waals separations. The parameter d_{norm} displays a surface with a red-white-blue color design, where bright red spots highlight shorter contacts, white areas in the same surface represent contacts around the van der Waals separation and the blue regions are devoid of close contacts [38].

3. Results and discussion

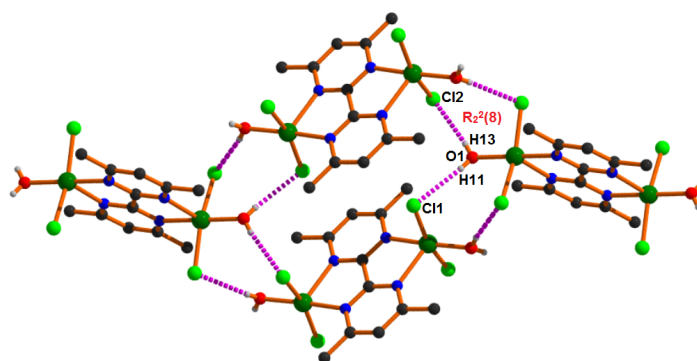
Single-crystal X-ray structural analysis confirms that the Cu(II) complex consists of a substituted bipyrimidine-bridged binuclear entity having the formula [Cu₂LCl₄(H₂O)₂] (**1**) with a ligand (L: 4,4',6,6'-Tetramethyl 2,2'-bipyrimidine), chloride ions and solvent water molecules. In this neutral complex, each copper(II) center adopts a square pyramidal geometry exploiting one nitrogen of the ligand moiety, two chloride ions, and one oxygen atoms of the coordinated water in an equatorial and another nitrogen atom of substituted bipyrimidine occupies at the apical position. The ligand forms a five-membered chelate ring around each central Cu(II) center.

Table 2. Bond distances and angles for complex 1.

Atom	Atom	Length (Å)	Atom	Atom	Length (Å)		
Cu1	Cl1	2.2773(7)	N1	C1	1.333(3)		
Cu1	Cl2	2.2748(7)	N1	C4	1.347(3)		
Cu1	N2 ¹	2.2748(18)	C3	C2	1.379(4)		
Cu1	N1	2.0105(19)	C3	C4	1.383(4)		
Cu1	O1	1.960(2)	C1	C1 ¹	1.491(4)		
N2	Cu1 ¹	2.2748(18)	C2	C6	1.486(4)		
N2	C1	1.328(3)	C4	C5	1.489(4)		
N2	C2	1.350(3)					
Atom	Atom	Atom	Angles (°)	Atom	Atom	Atom	Angles (°)
Cl2	Cu1	Cl1	163.55(3)	C1	N1	Cu1	118.33(15)
N2 ¹	Cu1	Cl1	97.91(5)	C1	N1	C4	117.7(2)
N2 ¹	Cu1	Cl2	98.03(5)	C4	N1	Cu1	123.71(16)
N1	Cu1	Cl1	91.45(5)	C2	C3	C4	120.0(2)
N1	Cu1	Cl2	87.93(5)	N2	C1	N1	125.96(19)
N1	Cu1	N2 ¹	77.85(7)	N2	C1	C1 ¹	117.3(2)
O1	Cu1	Cl1	90.40(8)	N1	C1	C1 ¹	116.7(2)
O1	Cu1	Cl2	88.93(8)	N2	C2	C3	119.8(2)
O1	Cu1	N2 ¹	106.67(10)	N2	C2	C6	118.0(2)
O1	Cu1	N1	174.84(10)	C3	C2	C6	122.2(2)
C1	N2	Cu1 ¹	109.48(13)	N1	C4	C3	119.3(2)
C1	N2	C2	117.26(19)	N1	C4	C5	118.1(2)
C2	N2	Cu1 ¹	133.22(16)	C3	C4	C5	122.7(2)

¹ 2-x, -y, -z.**Table 3.** Details of hydrogen bond distances (Å) and angles (°) for complex 1.

D-H...A	D (D-H) (Å)	D (H...A) (Å)	D(D...A) (Å)	∠ DHA (°)	Symmetry
O1-H11...Cl1	0.72(5)	2.47(5)	3.161(3)	161(5)	5/2-x, -1/2+y, 1/2-z
O1-H13...Cl2	0.66(4)	2.42(4)	3.077(3)	172(4)	5/2-x, 1/2+y, 1/2-z

**Figure 2.** 2D architecture utilizing the hydrogen bonding interactions in complex 1.

3.1. Structural description of complex 1

The molecular structure of complex 1 with the atom numbering scheme is shown in Figure 1, while its bond lengths and angles are listed in Table 2. Complex 1 crystallizes in a monoclinic system with the space group $P2_1/n$ and its unit cell contains four molecules. Complex 1 is a symmetric binuclear species comprising neutral $[\text{Cu}_2(\text{L})(\text{H}_2\text{O})_2\text{Cl}_2]$ where 'L' is 4,4', 6,6'-tetramethyl 2,2'-bipyrimidine compound. The symmetry adopted Cu(II) ions are placed in a square pyramidal pocket having the τ value is 0.19 (ideally $\tau = 1$ for the trigonal bipyramidal geometry and $\tau = 0$ for the square pyramidal geometry) [39] where the equatorial plane around each Cu(II) is constituted by one pyrimidyl nitrogen (N1), two chloride ions (Cl1 and Cl2) and one oxygen (O1) of coordinated water molecules while the apical position is occupied by another nitrogen atom (N2) of the substituted bipyrimidine system.

In complex 1, each Cu(II) ion is shifted by a distance of 0.202 Å towards the apical pyrimidine nitrogen (N2) from the equatorial mean plane N1/Cl1/O1/Cl2. Here, the title ligand acts as a bis-bidentate manner and acts as a connector between two copper centres separated by a distance of 5.693 Å. The equatorial Cu-Cl distances are almost the same (Cu1-Cl1 = 2.277(7) and Cu1-Cl2 = 2.2748(7) Å) while the Cu-N_{axial} bond distance (2.2748(18) Å) is larger compared to the Cu-N_{equatorial}

bond distance (2.0105(19) Å), which is quite usual due to the utilization of a lower *s* character of the orbital involved in the coordination. The average axial-equatorial and equatorial-equatorial (*cis*) bond angles are 95.11 and 89.67°, respectively (Table 2). Equatorial trans angles (N1-Cu1-O1 = 174.84(10) and Cl1-Cu1-Cl2 = 163.55(3)°) are deviated from the ideal trans angle 180° due to stereo-electronic obligations. The electrical charge of the copper (II) centres is taken care by four coordinated chloride ions.

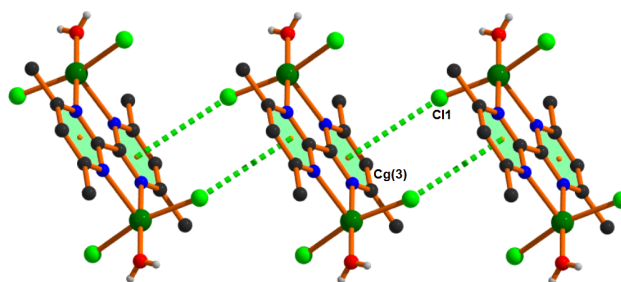
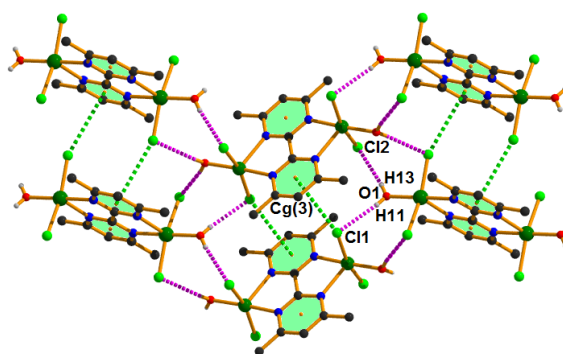
The crystal structure of complex 1 is stabilized through classical intermolecular O-H...Cl (between hydrogen of coordinated water and equatorially coordinated chloride ions) hydrogen bonding interactions (O1-H11...Cl1 and O1-H13...Cl2) (Figure 2, Table 3) and helped to construct a 2D architecture utilizing $R_2^2(8)$ supramolecular synthons. Therefore, it is the perfect self-assembly of a $[\text{Cu}_2\text{LCl}_4(\text{H}_2\text{O})_2]$ coordination motif held together by O-H...Cl hydrogen bonding interactions. In this 2D arrangement, the water molecule bearing one complex unit forms two O-H...Cl hydrogen bonding interactions simultaneously with the other two complex units (one provides Cl1 and another Cl2) of an almost parallel plane.

In structure of complex 1, between two coordinated chloride ions around each copper center, Cl1 is located above and below the electron deficient bipyrimidine ring (electron deficiency is generated from coordination to the central copper

Table 4. Geometric features (distances in Å and angles in degrees) of lone pair... π interaction obtained for complex **1**.

Lone pair...Cg	Lone pair...Cg (Å)	Lone pair...Perp (Å)	γ (°)	Cu-Cl...Cg (°)	Symmetry
Cu1-Cl1...Cg(3)*	3.7421(11)	3.389	25.1	151.91(3)	2-x, 1-y, -z

* Cg(3) = Centre of gravity of ring N1/C1/N2/C2/C3/C4.

**Figure 3.** 1D architecture of lone pair... π interaction in complex **1**.**Figure 4.** 2D architecture combining the hydrogen bonding interaction and the lone pair... π interaction in complex **1**.

(II) ion) to form an effective lone pair... π interaction and generate a one-dimensional architecture (Figure 3). To the best of our knowledge, it is the first report of lone pair... π interaction using the title ligand 4,4',6,6'-tetramethyl 2,2'-bipyrimidine.

This one-dimensional architecture formed by the lone pair... π interaction extends the dimensionality to 2D (Figure 4, Table 4) in association with intermolecular hydrogen bonding interactions (between equatorially coordinated chlorides and the hydrogen atoms of the coordinated water molecules).

3.2. Hirshfeld surface analysis

The Hirshfeld surface analyses of the complex **1** was carried out on its asymmetric unit to quantify the intermolecular interactions and to provide a detailed account of the supra-molecular assembly by hydrogen bonding and lone pair... π interactions. The crystallographic information file (CIF) was used as the input to generate the Hirshfeld surfaces and fingerprint plots using CrystalExplorer program. The red-blue-white color scheme is utilized for quantifying the interactions and provides a resource to analyze the strength of the contacts. The Hirshfeld surfaces of the title complex are mapped over the d_{norm} (range: -0.29 to 1.13 Å), d_e , d_i , and shape index (Figure 5). The shape-index surface has been shown to convey information about each donor-acceptor pair in the complex. The surfaces are made transparent to enable visualization of the molecular moiety around which they are calculated. The shape index curve exhibits complementary red (pit) - blue (bump) that correspond to the negative and positive surface property value, respectively, the former representing the location of an acceptor atom and the latter pointing towards a donor atom. The dominant interactions observed in complex **1** are H...H (41.2%), H...Cl (39.8%), H...C (7.9%) and C...Cl (5.5%) which appear as red spots on the d_{norm} surface in Figure 5.

Furthermore, the 2D fingerprint plots represent all intermolecular interactions that are involved within the structures. To quantify each individual contact, we have demonstrated the full fingerprint plots in unique visual mode. The intermolecular interactions appear as distinct spikes in the 2D fingerprint plot showing the different spikes with their corresponding interactions. Figure 6 represents the 2D fingerprint plot for hydrogen bonding interactions. Figure 7 represent the Hirshfeld surface view of d_{norm} and curvedness of O-H...Cl hydrogen bonding interaction. Figure 8 represents the 2D fingerprint plot for lone pair... π interactions in complex **1**. Figure 9 represents the Hirshfeld surface view of the d_{norm} and the curvedness of the lone pair... π interactions in complex **1**. Figure 10 represents the fingerprint plots of all interactions, H...H interaction and C...H interaction in complex **1**.

The H...Cl/Cl...H interactions appear as two distinct spikes in the fingerprint plot and comprise 39.8% of the total Hirshfeld surface for complex **1**. The H...C/C...H and C...Cl/Cl...C interactions contribute 7.9 and 5.5%, respectively, whereas the contribution H...H/H...H interactions is 41.2% to the total surface area of the complex. This analysis quantifies the intermolecular interactions involved within the crystal structure by providing a full understanding of these interactions in a facile way.

The method allowed calculation of energies based on unperturbed electron distributions computed at the B3LYP level of theory employing the 6-31G(d,p) basis set. As complex **1** contains no atoms heavier than krypton, the 6-31G basis set was used and the total energy E_{tot} (kJ/mol), which is the sum of four contributing factors, electrostatic (E_{ele}), polarization (E_{pol}), dispersion (E_{dis}) [40-42] and exchange repulsion (E_{rep}) was calculated for pairs of molecules (Table 5).

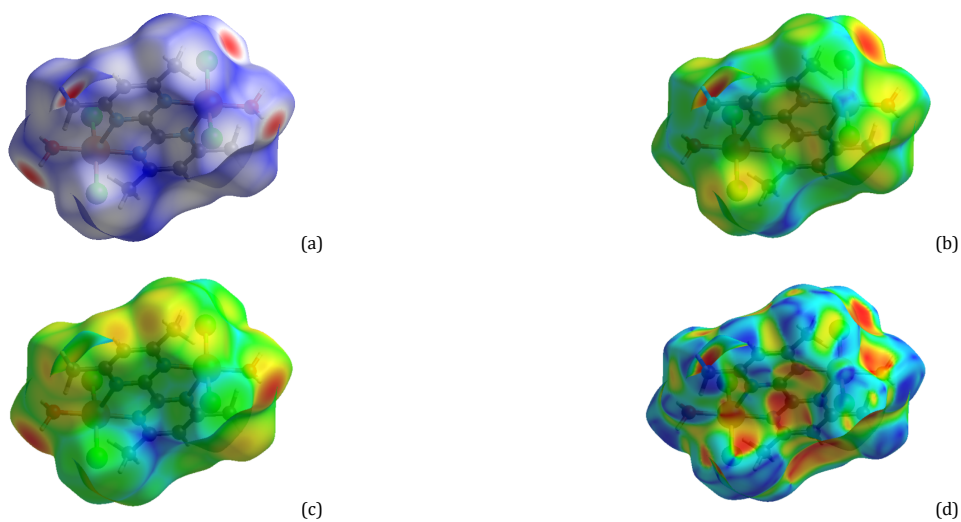


Figure 5. Hirshfeld surfaces mapped with (a) d_{norm} , (b) d_e , (c) d_i , and (d) shape-index for complex 1.

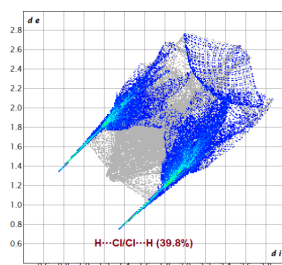


Figure 6. Fingerprint plot for hydrogen bonding interaction in complex 1.

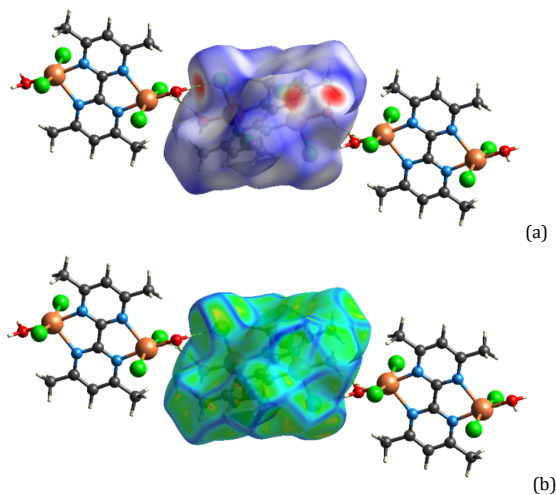


Figure 7. The Hirshfeld surface view in (a) d_{norm} and (b) curvedness showing the prominent O-H...Cl hydrogen bonding interaction.

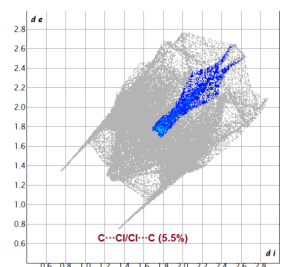
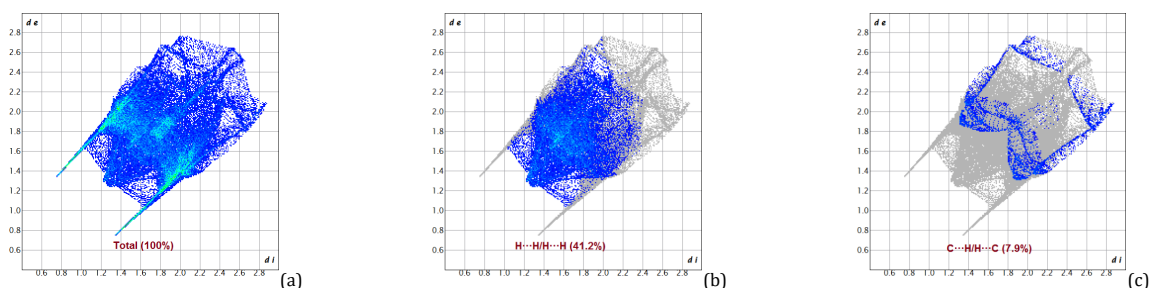
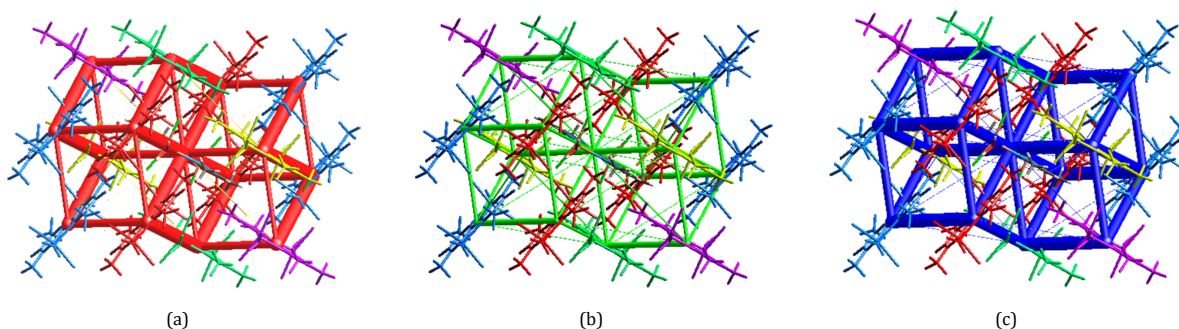


Figure 8. Fingerprint plot for lone pair... π interactions in complex 1.

Table 5. Interaction energies of complex 1 using Crystal Explorer in kJ/mol.

Color	N	Symop	R	E_{ele}	E_{pol}	E_{dis}	E_{rep}	E_{tot}
Red	4	$-x+1/2, y+1/2, -z+1/2$	9.92	-104.2	-32.9	-25.6	83.3	-83.1
Yellow	2	x, y, z	7.65	-61.1	-25.3	-52.2	31.0	-100.7
Green	2	x, y, z	7.22	-36.8	-21.8	-32.7	21.2	-64.0
Blue	4	$-x+1/2, y+1/2, -z+1/2$	10.77	0.5	-4.9	-8.0	6.8	-4.5
Purple	2	x, y, z	10.51	6.8	-3.3	-15.2	4.4	-5.4

**Figure 9.** The Hirshfeld surface view in (a) d_{norm} and (b) curvedness shows the prominent lone pair... π interactions in complex 1.**Figure 10.** Fingerprint plots (a) Full, (b) H...H, and (c) H...C interaction in complex 1.**Figure 11.** Energy framework showing (a) the electrostatic potential force (Coulomb energy), (b) the dispersion force and (c) the total energy diagrams in a $1 \times 1 \times 1$ unit cell. The radii of the cylinders were proportional to the relative strength of the energy and was adjusted to the same scale factor of 50 with a cut-off value of 0 kJ/mol.

The total energy is delineated into the electrostatic potential energy/Coulomb energy, polarization energy, dispersion energy due to the van der Waals interaction, and the repulsion energy. The total energies, only reported for two

benchmarked energy models, are the sum of the four energy components, scaled appropriately. The scale factors employed for the CE-B3LYP...B3LYP/6-31G(d,p) are $k_{ele} = 1.057$, $k_{pol} = 0.740$, $k_{disp} = 0.871$, $k_{rep} = 0.618$.

The energy frameworks were simulated to give a visual understanding of the individual components' contribution to the total energy through cylinders that joined the interacting pairs of molecules. The radius of the cylinder was fixed at 50 kJ/mol to quantify the contributing energies, and a suitable cut-off (0 kJ/mol) was chosen for clarity purposes. A 1×1×1 unit cell was selected for the creation of a cluster. The red, green, and blue cylinders were used to depict E_{ele} , E_{dis} , and E_{tot} , respectively (Figure 11). This approach allowed for the evaluation of the mechanical behavior of the complex at the molecular level and proved significant in terms of crystal engineering. The thickness of the cylinders is comparable to the relative strength of the interaction energy. For the studied cluster, the total electrostatic energy is -194.8 kJ/mol, dispersion energy is -133.7 kJ/mol, polarization energy is -88.2 kJ/mol, repulsion energy is 146.7 kJ/mol and the total interaction energy is -257.7 kJ/mol. The results reveal the electrostatic energy as the major component in stabilizing the molecular structure of complex 1 in solid state.

4. Conclusions

A new binuclear copper (II) complex $[Cu_2L_2Cl_4(H_2O)_2]$ (**1**) has been synthesized using a 4,4',6,6'-tetramethyl 2,2'-bipyrimidine ligand in aqueous methanol solvent and characterized by elemental, spectral and single-crystal X-ray crystallographic analysis. Complex **1** is distorted square pyramidal and crystallizes in a monoclinic system with the space group $P2_1/n$. The ligand acts as a bis-bidentate one using the four nitrogen donor centers and bridges two copper (II) centers separated by a distance of 5.693 Å. The complex is stabilized by classical O-H...Cl intermolecular hydrogen bonding interaction utilizing coordinated water and equatorially coordinated two chloride ions. By exploiting such interaction complex **1** generates a 2D supramolecular architecture. The charge-assisted terminal chloride ions interact with electronically poor π -rings of pyrimidine, and such a lone pair... π interaction provides a 1D chain, which in turn enhances its dimensionality in association with O-H...Cl hydrogen bonding interaction. Hirshfeld surface analysis was carried out to quantify the interactions and an interaction energy analysis was performed to study the interactions between pairs of molecules. The 2D fingerprint plots associated with the Hirshfeld surface unambiguously prove the existence of each significant interaction involved in the structure by quantifying them in an effective visual manner. The calculation of the interaction energy depicts the dominance of the electrostatic energy in the stabilization of complex **1** in the solid state.

Acknowledgements

Samit Pramanik is grateful to the Council of Scientific and Industrial Research (CSIR, File no. 09/096(0947)/2018-EMR-I), New Delhi, for a Senior Research Fellowship.

Supporting information

CCDC-2192141 contains the supplementary crystallographic data for this paper. These data can be obtained free of charge via <https://www.ccdc.cam.ac.uk/structures/>, or by e-mailing data_request@ccdc.cam.ac.uk, or by contacting The Cambridge Crystallographic Data Centre, 12 Union Road, Cambridge CB2 1EZ, UK; fax: +44(0)1223-336033.

Disclosure statement

Conflict of interest: The authors have no conflict of interest to declare that is relevant to the content of this paper.

Ethical approval: All ethical guidelines have been adhered.

Sample availability: Samples of the compounds are available from the author.

CRedit authorship contribution statement

Conceptualization: Subrata Mukhopadhyay and Kinsuk Das; Methodology: Subrata Mukhopadhyay and Kinsuk Das; Software: Samit Pramanik; Validation: Samit Pramanik and Kinsuk Das; Formal Analysis: Samit Pramanik and Kinsuk Das; Investigation: Samit Pramanik and Kinsuk Das; Resources: Samit Pramanik and Kinsuk Das; Data Curation: Samit Pramanik and Kinsuk Das; Writing - Original Draft: Kinsuk Das; Writing - Review and Editing: Samit Pramanik and Kinsuk Das; Visualization: Kinsuk Das; Funding acquisition: Samit Pramanik; Supervision: Subrata Mukhopadhyay and Kinsuk Das; Project Administration: Subrata Mukhopadhyay.

ORCID and Email

Samit Pramanik

 samit.chemistry94@gmail.com

 <https://orcid.org/0000-0002-0408-9386>

Subrata Mukhopadhyay

 ju_subrata@yahoo.co.in

 <https://orcid.org/0000-0001-7993-7426>

Kinsuk Das

 kdaschem@yahoo.in

 <https://orcid.org/0000-0002-7717-8734>

References

- Sinnokrot, M. O.; Valeev, E. F.; Sherrill, C. D. Estimates of the ab initio limit for π - π interactions: The benzene dimer. *J. Am. Chem. Soc.* **2002**, *124*, 10887–10893.
- Alkorta, I.; Elguero, J.; Frontera, A. Not only hydrogen bonds: Other noncovalent interactions. *Crystals (Basel)* **2020**, *10*, 180.
- Noncovalent Forces*; Scheiner, S., Ed.; Springer International Publishing: Cham, Switzerland, 2016.
- Mahadevi, A. S.; Sastry, G. N. Cooperativity in noncovalent interactions. *Chem. Rev.* **2016**, *116*, 2775–2825.
- Alkorta, I.; Blanco, F.; Deyà, P. M.; Elguero, J.; Estarellas, C.; Frontera, A.; Quiñero, D. Cooperativity in multiple unusual weak bonds. *Theor. Chem. Acc.* **2010**, *126*, 1–14.
- Bauzá, A.; Mooibroek, T. J.; Frontera, A. Small cycloalkane (CN)2C@C(CN)2 structures are highly directional non-covalent carbon-bond donors. *Chemistry* **2014**, *20*, 10245–10248.
- Mitra, M.; Manna, P.; Bauzá, A.; Ballester, P.; Seth, S. K.; Ray Choudhury, S.; Frontera, A.; Mukhopadhyay, S. 3-picoline mediated self-assembly of M(II)-malonate complexes (M = Ni/co/Mn/mg/Zn/cu) assisted by various weak forces involving lone pair- π , π - π , and anion... π -hole interactions. *J. Phys. Chem. B* **2014**, *118*, 14713–14726.
- Bauzá, A.; Mooibroek, T. J.; Frontera, A. Directionality of π -holes in nitro compounds. *Chem. Commun. (Camb.)* **2015**, *51*, 1491–1493.
- Non-covalent interactions in the synthesis and design of new compounds: Maharramov/non-covalent interactions in the synthesis and design of new compounds*; Maharramov, A. M.; Mahmudov, K. T.; Kopylovich, M. N.; Pombeiro, A. J. L., Eds.; John Wiley & Sons: Nashville, TN, 2016.
- Pal, P.; Das, K.; Hossain, A.; Frontera, A.; Mukhopadhyay, S. Supramolecular and theoretical perspectives of 2,2':6',2''-terpyridine based Ni(II) and Cu(II) complexes: on the importance of C-H...Cl and π ... π interactions. *New J Chem* **2020**, *44*, 7310–7318.
- Das, K.; Dolai, M.; Chatterjee, S.; Konar, S. Synthesis, X-ray crystal structure and BVS calculation of Co(II) complex of pyrimidine derived Schiff base ligand: Approached by Hirshfeld surface analysis and TDDFT calculation. *J. Mol. Struct.* **2021**, *1236*, 130269.
- Pal, P.; Das, K.; Hossain, A.; Gomila, R. M.; Frontera, A.; Mukhopadhyay, S. Synthesis and crystal structure of the simultaneous binding of Ni(II) cation and chloride by the protonated 2,4,6 tris-(2-pyridyl)-1,3,5 triazine ligand: theoretical investigations of anion... π , π ... π and hydrogen bonding interactions. *New J Chem* **2021**, *45*, 11689–11696.
- Kitagawa, S.; Matsuda, R. Chemistry of coordination space of porous coordination polymers. *Coord. Chem. Rev.* **2007**, *251*, 2490–2509.
- Perry, J. J., IV; Perman, J. A.; Zawortko, M. J. Design and synthesis of metal-organic frameworks using metal-organic polyhedra as supermolecular building blocks. *Chem. Soc. Rev.* **2009**, *38*, 1400–1417.
- Biswas, C.; Drew, M. G. B.; Escudero, D.; Frontera, A.; Ghosh, A. Anion- π , lone-pair- π , π - π and hydrogen-bonding interactions in a cu II complex of 2-picolinate and protonated 4,4'-bipyridine: Crystal structure and theoretical studies. *Eur. J. Inorg. Chem.* **2009**, *2009*, 2238–2246.
- Andruh, M. Oligonuclear complexes as tectons in crystal engineering: structural diversity and magnetic properties. *Chem. Commun. (Camb.)* **2007**, 2565–2577.

- [17]. Pointillart, F.; Herson, P.; Boubekeur, K.; Train, C. Square-planar and trigonal prismatic silver(I) in bipyrimidine and oxalate bridged tetranuclear complexes and one-dimensional compounds: Synthesis and crystal structures. *Inorganica Chim. Acta* **2008**, *361*, 373–379.
- [18]. Ma, N.; Wang, Y. Crystal structure of tetraaqua dinitrato- κ 2O, O'-4,4',6,6'-tetramethyl-2,2'-bipyrimidine- κ 4N, N':N'', N''' dinickel(II) dinitrate, C₆H₁₁N₄NiO₈. *Z. Krist. - New Cryst. Struct.* **2014**, *229*, 109–110.
- [19]. Naiya, S.; Biswas, C.; Drew, M. G. B.; Gómez-García, C. J.; Clemente-Juan, J. M.; Ghosh, A. A unique example of structural and magnetic diversity in four interconvertible copper(II)–Azide complexes with the same Schiff base ligand: A monomer, a dimer, a chain, and a layer. *Inorg. Chem.* **2010**, *49*, 6616–6627.
- [20]. Das, K.; Mandal, T. N.; Roy, S.; Jana, A.; Konar, S.; Liu, C.-M.; Barik, A. K.; Kar, S. K. Syntheses, crystal structures and magnetic properties of two dicopper(II) complexes and a zigzag 1-D Cu(II) complex of a bidentate pyridyl-pyrazole ligand. *Polyhedron* **2011**, *30*, 715–724.
- [21]. Luo, J.; Zhang, X.-R.; Gao, E.-Q.; Dai, W.-Q.; Cui, L.-L.; Liu, B.-S. Syntheses, structures and magnetic properties of two copper(II) tricyano methanide complexes with 2,2'-bipyrimidine as bridging ligands. *Inorganica Chim. Acta* **2009**, *362*, 1749–1754.
- [22]. Marino, N.; Armentano, D.; De Munno, G.; Cano, J.; Lloret, F.; Julve, M. Synthesis, Structure, and Magnetic Properties of Regular Alternating μ -bpm/di- μ -X Copper(II) Chains (bpm = 2,2'-bipyrimidine; X = OH, F). *Inorg. Chem.* **2012**, *51*, 4323–4334.
- [23]. Ma, N.; Wang, Y.; Miao, S.-B. Crystal structure of tetraaqua diacetato- κ 2O, O'-4,4',6,6'-tetramethyl-2,2'-bipyrimidine- κ 4N, N':N'', N''' dicobalt(II) diacetate dihydrate, C₁₀H₁₉CoN₂O₇. *Z. Krist. - New Cryst. Struct.* **2014**, *229*, 107–108.
- [24]. Williams, R. M.; Cola, L. D.; Hartl, F.; Lagref, J.-J.; Planeix, J.-M.; Cian, A. D.; Hosseini, M. W. Photophysical, electrochemical and electrochromic properties of copper-bis(4,4'-dimethyl-6,6'-diphenyl-2,2'-bipyridine) complexes. *Coord. Chem. Rev.* **2002**, *230*, 253–261.
- [25]. Chandrasekaran, R.; Murugavel, S.; Guin, M.; Silambarasan, T. Crystal structure, Hirshfeld, computational biomolecular investigations, and MTT assay studies of amino pyrimidine derivative as EGFR kinase domain inhibitor. *J. Mol. Struct.* **2022**, *1254*, 132416.
- [26]. Rajni Swamy, V.; Krishnakumar, R. V.; Srinivasan, N.; Sivakumar, S.; Kumar, R. R. Coordinated compliance of chloro-methyl and bromomethyl exchange rule in two dihydrofuran carbonitrile derivatives. *J. Mol. Struct.* **2021**, *1228*, 129741.
- [27]. Pramanik, S.; Pathak, S.; Frontera, A.; Mukhopadhyay, S. Syntheses, crystal structures and supramolecular assemblies of two Cu(ii) complexes based on a new heterocyclic ligand: insights into C–H...Cl and π ... π interactions. *CrystEngComm* **2022**, *24*, 1598–1611.
- [28]. Vlád, G.; Horváth, I. T. Improved synthesis of 2,2'-bipyrimidine. *J. Org. Chem.* **2002**, *67*, 6550–6552.
- [29]. Bruker (2001). SMART. Bruker AXS Inc., Madison, Wisconsin, USA.
- [30]. Sheldrick, G. M. (1997). SHELXS-97 and SHELXL-97. University of Göttingen, Germany.
- [31]. Spackman, M. A.; Jayatilaka, D. Hirshfeld surface analysis. *CrystEngComm* **2009**, *11*, 19–32.
- [32]. Hirshfeld, F. L. Bonded-atom fragments for describing molecular charge densities. *Theoret. Chim. Acta* **1977**, *44*, 129–138.
- [33]. Clausen, H. F.; Chevallier, M. S.; Spackman, M. A.; Iversen, B. B. Three new co-crystals of hydroquinone: crystal structures and Hirshfeld surface analysis of intermolecular interactions. *New J Chem* **2010**, *34*, 193–199.
- [34]. Rohl, A. L.; Moret, M.; Kaminsky, W.; Claborn, K.; McKinnon, J. J.; Kahr, B. Hirshfeld surfaces identify inadequacies in computations of intermolecular interactions in crystals: Pentamorphic 1,8-dihydroxyanthraquinone. *Cryst. Growth Des.* **2008**, *8*, 4517–4525.
- [35]. Parkin, A.; Barr, G.; Dong, W.; Gilmore, C. J.; Jayatilaka, D.; McKinnon, J. J.; Spackman, M. A.; Wilson, C. C. Comparing entire crystal structures: structural genetic fingerprinting. *CrystEngComm* **2007**, *9*, 648–652.
- [36]. Spackman, M. A.; McKinnon, J. J. Fingerprinting intermolecular interactions in molecular crystals. *CrystEngComm* **2002**, *4*, 378–392.
- [37]. Spackman, P. R.; Turner, M. J.; McKinnon, J. J.; Wolff, S. K.; Grimwood, D. J.; Jayatilaka, D.; Spackman, M. A. CrystalExplorer: a program for Hirshfeld surface analysis, visualization and quantitative analysis of molecular crystals. *J. Appl. Crystallogr.* **2021**, *54*, 1006–1011.
- [38]. McKinnon, J. J.; Spackman, M. A.; Mitchell, A. S. Novel tools for visualizing and exploring intermolecular interactions in molecular crystals. *Acta Crystallogr. B* **2004**, *60*, 627–668.
- [39]. Addison, A. W.; Rao, T. N.; Reedijk, J.; van Rijn, J.; Verschoor, G. C. Synthesis, structure, and spectroscopic properties of copper(II) compounds containing nitrogen–sulphur donor ligands; the crystal and molecular structure of aqua[1,7-bis(N-methylbenzimidazol-2'-yl)-2,6-dithiaheptane]copper(II) perchlorate. *J. Chem. Soc., Dalton Trans.* **1984**, 1349–1356.
- [40]. Swamy, R.; Ravikumar. Crystal structure determination, hirshfeld surface analysis and quantum computational studies of (3E,5E)-1-ethyl-3,5-bis(naphthalen-1-yl-methylidene) piperidin-4-one: A novel RORc inhibitor. *J. Mol. Struct.* **2021**, *1225*, 129313.
- [41]. Turner, M. J.; Thomas, S. P.; Shi, M. W.; Jayatilaka, D.; Spackman, M. A. Energy frameworks: insights into interaction anisotropy and the mechanical properties of molecular crystals. *Chem. Commun. (Camb.)* **2015**, *51*, 3735–3738.
- [42]. Mackenzie, C. F.; Spackman, P. R.; Jayatilaka, D.; Spackman, M. A. CrystalExplorer model energies and energy frameworks: extension to metal coordination compounds, organic salts, solvates and open-shell systems. *IUCr* **2017**, *4*, 575–587.



Copyright © 2022 by Authors. This work is published and licensed by Atlanta Publishing House LLC, Atlanta, GA, USA. The full terms of this license are available at <http://www.eurjchem.com/index.php/eurjchem/pages/view/terms> and incorporate the Creative Commons Attribution-Non Commercial (CC BY NC) (International, v4.0) License (<http://creativecommons.org/licenses/by-nc/4.0>). By accessing the work, you hereby accept the Terms. This is an open access article distributed under the terms and conditions of the CC BY NC License, which permits unrestricted non-commercial use, distribution, and reproduction in any medium, provided the original work is properly cited without any further permission from Atlanta Publishing House LLC (European Journal of Chemistry). No use, distribution or reproduction is permitted which does not comply with these terms. Permissions for commercial use of this work beyond the scope of the License (<http://www.eurjchem.com/index.php/eurjchem/pages/view/terms>) are administered by Atlanta Publishing House LLC (European Journal of Chemistry).